Vibrational Circular Dichroism, Predominant Conformations, and Hydrogen Bonding in (*S*)-(−)-3-Butyn-2-ol

Feng Wang and Prasad L. Polavarapu*

Department of Chemistry, Vanderbilt University, Nashville, Tennessee 37235

Received: July 26, 1999; In Final Form: November 5, 1999

Vibrational absorption and circular dichroism spectra of (*S*)-(−)-3-butyn-2-ol have been measured in CCl_4 solutions in the 2000−900 cm^{-1} region. Experimental spectra obtained at different concentrations are compared with the ab initio predictions of absorption and VCD spectra obtained with density functional theory using B3LYP/6-31G* basis set for three different conformers of (*S*)-(−)-3-butyn-2-ol. The Boltzmann populations, obtained from Gibbs free energies, indicate the presence of two predominant conformations for the isolated molecule. The population-weighted theoretical spectra are in satisfactory agreement with the experimental spectra obtained at dilute concentrations. The influence of intermolecular hydrogen bonding is seen in the experimental spectra at higher concentrations, where a single conformation appears to be predominant. A vibrational analysis was also undertaken for all three conformers and vibrational assignments were proposed for the observed bands.

Introduction

The interest in enantiomerically pure chemicals for medicinal use has increased recently, because the two enantiomers of chiral compounds in some cases have significantly different pharmaceutical effects.[1] To understand or model the molecular basis of pharmaceutical effect, determination of not only the absolute configuration but also the predominant conformations of a given chiral molecule is important. While traditional methods such as electronic circular dichroism[2] have widely been used for determining the absolute configuration of chiral compounds, the experimental and ab initio optical rotations are also being used[3] in recent years for this purpose. Vibrational optical activity (VOA) is another chiroptical method that is being developed since early 1970s and holds promise for determining complete molecular stereochemistry in the solution phase. There are two forms of VOA: one is infrared vibrational circular dichroism (VCD)[4] and the other is vibrational Raman optical activity (VROA).[5] These two techniques benefit from a large number of vibrational transitions that are accessible for stereochemical elucidation.

The absolute configuration and predominant conformations have successfully been determined[6−10] for several chiral molecules (including anesthetics and organic systems) by comparing the experimental VOA observations for a given enantiomer with those predicted using ab initio theoretical methods for a given configuration and different conformations.

The absolute configuration of (−)-3-butyn-2-ol (which is useful[11] as a material for drugs, agrochems, perfumes, and liquid crystals) has been known[12] to be (*S*). The microwave spectral studies[13] on 3-butyn-2-ol in the gas phase suggested the presence of two predominant conformations of 3-butyn-2-ol. Optical rotation calculations[14] suggested that one particular conformation is responsible for negative optical rotation of (*S*)-3-butyn-2-ol as neat liquid. This indicates differing conformations of 3-butyn-2-ol in different physical states. It is useful to have the experimental and theoretical data that would identify the conformations preferred by 3-butyn-2-ol in the solution phase.

Improvements in VCD instrumentation in recent years have made it possible to obtain the VCD spectra with enhanced signal-to-noise ratio. Ab initio applications using density functional theory (DFT),[15] have also become state of the art in recent years. So, the quantum mechanical energy calculations using DFT would be useful for determining the predominant conformations of 3-butyn-2-ol. No such calculations have been reported for 3-butyn-2-ol. The DFT theory, which provides vibrational frequencies and intensities that are comparable to the post-SCF calculations employing electron correlation, has also been extended to the VCD intensity calculations.[16] These developments make it possible to use VCD for a reliable determination of the absolute configuration and predominant conformations. Therefore, we have measured the VCD of (*S*)-(−)-3-butyn-2-ol and undertaken state of the art ab initio theoretical VCD investigations using the B3LYP/6-31G* basis set. These results are used for suggesting the predominant conformations of 3-butyn-2-ol.

There are no previous studies in the literature dealing with the vibrational analysis or vibrational assignments for the observed vibrational bands of 3-butyn-2-ol. Thus, we have also undertaken vibrational analysis for all three conformers of 3-butyn-2-ol, which permits us to suggest the assignments for the observed vibrational bands.

Procedures

(*S*)-(−)-3-Butyn-2-ol was purchased from Aldrich Chemical Co. The infrared and VCD spectra were recorded on a commercial Fourier transform VCD spectrometer, Chiralir (Bomem-BioTools, Canada) with a ZnSe beam splitter, BaF_2 polarizer, optical filter (transmitting below 2000 cm^{-1}), and a 2 × 2 mmHg CdTe detector. One difference from the standard Chiralir instrument is that the photoelastic modulator used was a PEM-80 model (Hinds Instruments) without AR coating on the ZnSe optical element. The VCD spectra were recorded using the supplied Chiralir software, with 3 h data collection time at 4 cm^{-1} resolution. The transmission properties of optical filter and BaF_2 substrates used in the instrument restrict the range of

10.1021/jp992576k CCC: $19.00
Published on Web 03/02/2000

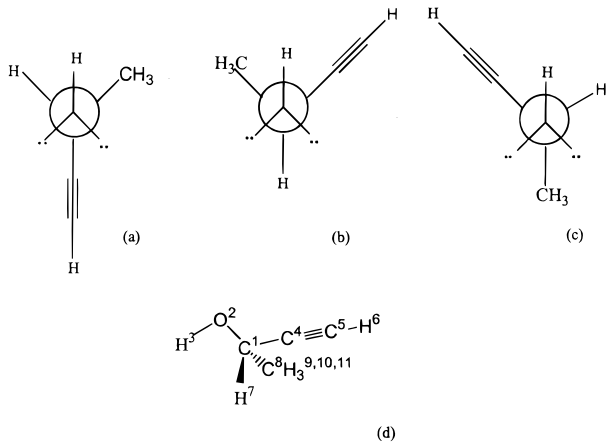

Figure 1. Different conformations of (*S*)-3-butyn-2-ol: (a) *trans*-acetylene conformation; (b) *trans*-H conformation; (c) *trans*-methyl conformation; (d) absolute configuration of (*S*)-3-butyn-2-ol with atom numbering used to define the internal coordinates in Table 3.

measurements to 2000−900 cm^{-1}. Spectra were measured in CCl_4 solvent at three different concentrations, 0.103, 0.308, and 0.858 M, at path length of ∼500, ∼200, or 80 μm, respectively. The sample was held in a variable path length cell with BaF_2 windows. In the presented absorption spectra, the solvent absorption was subtracted out. In the presented VCD spectra the raw VCD spectrum of the solvent was subtracted.

The ab initio vibrational frequencies and absorption and VCD intensities for (*S*)-(−)-3-butyn-2-ol were calculated using the Gaussian 98 program[17] on a Pentium II 300 MHz PC. The calculations used the density functional theory (DFT) with B3LYP functional[15−17] and 6-31G* basis set.[18] The procedure for calculating the VCD intensities using DFT theory is due to Cheeseman et al.[16] as implemented in the Gaussian 98 program.[17] The theoretical absorption and VCD spectra were simulated with Lorentzian band shapes and 10 cm^{-1} full width at half-height. Since the ab initio predicted band positions are higher than the experimental values, the ab initio frequencies were scaled with 0.96.

For the normal-coordinate analysis, the following procedure was used to transform the ab initio data. The Cartesian coordinates obtained for the optimized structure were input into the GMAT program[19] along with the definitions of internal coordinates. The **B**-matrix, obtained as the output, was then used to convert the ab initio Cartesian force constants to internal coordinate force constants. These internal coordinate force constants, along with the **B**-matrix, were used to calculate the potential energy distribution (PED) among the internal coordinates. The latter two calculations were done with the computer programs developed in our laboratory.

Results and Discussion

Three possible conformations of (*S*)-3-butyn-2-ol, differing in the dihedral angle H−O−C*−H (see Figure 1) and labeled as *trans*-H, *trans*-methyl, and *trans*-acetylene, are investigated. Using the starting H−O−C*−H dihedral angles of −60° for *trans*-acetylene, 180° for *trans*-H and +60° for *trans*-methyl conformations, the geometries were optimized with B3LYP/6-31G* basis set. The converged H−O−C*-H dihedral angles, optimized energies, and relative populations based on the Gibbs free energies are listed in Table 1. In the *trans*-H and *trans*-methyl conformations (see Figure 1), the O−H group is gauche to the acetylene moiety which permits intramolecular hydrogen bonding between the O−H group and π-electrons of the acetylene moiety. Such intramolecular hydrogen bonding is not possible in the *trans*-acetylene conformation. As a result, the *trans*-H and *trans*-methyl conformations have lower energies and higher populations than those of *trans*-acetylene conformation. Based on these relative populations, it can be concluded that the ab initio calculations predict the isolated 3-butyn-2-ol molecule to exist predominantly in two conformations, *trans*-H (52%) and *trans*-methyl (47%).

The structural parameters for all three conformers are listed in Table 2 and compared to those derived from microwave

TABLE 1: Conformations and Energies of 3-Butyn-2-ol

	H−O−C*−H geom[a] (deg)		energy[b]			
conformation	starting	converged	electronic	Gibbs	ΔE[c]	populn[d] (%)
trans-acetylene	−60	−60.4	−231.168 89	−231.108 35	1.965	1.9
trans-H	180	172.1	−231.172 06	−231.111 48	0.0	52.4
trans-methyl	60	69.4	−231.171 95	−231.111 35	0.082	45.7

[a] Dihedral angle. [b] In hartrees. [c] Relative energy difference (in kcal/mol). [d] Percent population based on Gibbs energies.

TABLE 2: Structural Parameters of 3-Butyn-2-ol[a]

	trans-acetylene		*trans*-H		*trans*-methyl	
parameter	microwave	ab initio	microwave	ab initio	microwave	ab initio
C−C		1.206	1.206	1.208	1.206	1.208
C−CC		1.467	1.460	1.473	1.460	1.473
C−C		1.536	1.535	1.536	1.535	1.529
C−O		1.431	1.415	1.429	1.415	1.430
H−C		1.066	1.060	1.067	1.060	1.067
H−C		1.095	1.093	1.095	1.093	1.094
H−O		0.971	0.950	0.971	0.950	0.970
H−CC		179.3	180.0	179.2	180.0	178.9
CC−C		178.2	180.0	178.0	180.0	178.1
C−C−O		107.8	112.5	111.6	112.5	111.5
C−C−H		108.6	109.5	108.8	109.5	107.9
H−C−H		108.1	109.5	109.1	109.5	109.2
C−C−CH3		111.3	110.5	111.5	112.0	112.3
O−C−CH3		111.4	112.5	111.6	108.1	106.7
C−C−O−H		−177.6	45	54.8	56	50.2

[a] Microwave data are from ref 13; ab initio results are obtained with B3LYP/6-31G* basis sets; bond lengths are in angstrom units and bond angles are in degrees.

TABLE 3: Internal Coordinate[a] Definitions for 3-Butyn-2-ol

no.	coordinate	no.	coordinate	no.	coordinate
1	C_1O_2 stretch	10	C_8H_{11} stretch	19	$H_9C_8H_{10}$ bend
2	C_1C_4 stretch	11	$O_2C_1C_8$ bend	20	$H_9C_8H_{11}$ bend
3	C_1H_7 stretch	12	$O_2C_1H_7$ bend	21	$C_1O_2H_3$ bend
4	C_1C_8 stretch	13	$O_2C_1C_4$ bend	22	$C_1C_4C_5$ bend
5	O_2H_3 stretch	14	$C_8C_1C_4$ bend	23	$C_4C_5H_6$ bend
6	C_4C_5 stretch	15	$H_7C_1C_4$ bend	24	$C_8C_1O_2H_3$ torsion
7	C_5H_6 stretch	16	$C_1C_8H_9$ bend	25	$H_9C_8C_1O_2$ torsion
8	C_8H_9 stretch	17	$C_1C_8H_{10}$ bend	26	$C_5C_4C_1O_2$ torsion
9	C_8H_{10} stretch	18	$C_1C_8H_{11}$ bend	27	$H_6C_5C_4C_1$ torsion

[a] For atom numbering see Figure 1. As the C1−C4−C5−H6 segment is not perfectly linear (see Table 2), linear bending coordinates were not defined for this segment.

spectral data.[13] Although the microwave spectral data were fitted only to the angles C−C−CH_3, O−C−CH_3, and C−C−O−H, while keeping the other structural parameters fixed, they are very close to the predicted structural parameters.

All three conformers investigated were found to have energy minima (that is, all vibrational frequencies are real) at the B3LYP/6-31G* level, so the absorption and VCD intensities were calculated for all of them at the B3LYP/6-31G* level. The vibrational assignments, based on the internal coordinates defined in Table 3, are given in Table 4. The listed calculated frequencies in Table 5 correspond to the peak maxima in the simulated, population weighted, theoretical absorption spectra so the fundamentals are assigned predominantly for the *trans*-H (52%) and *trans*-methyl (47%) conformers. The predicted frequencies (calculated frequencies scaled with 0.96) are reasonably close to the observed frequencies. The predicted absorption and VCD spectra simulated with 10 cm^{-1} half-widths and Lorentzian band shapes are shown in Figures 2 and 3. The theoretical spectra obtained for (*S*)-3-butyn-2-ol are compared to the experimental spectra of (−)-3-butyn-2-ol, at different concentrations, in Figures 4 and 5.

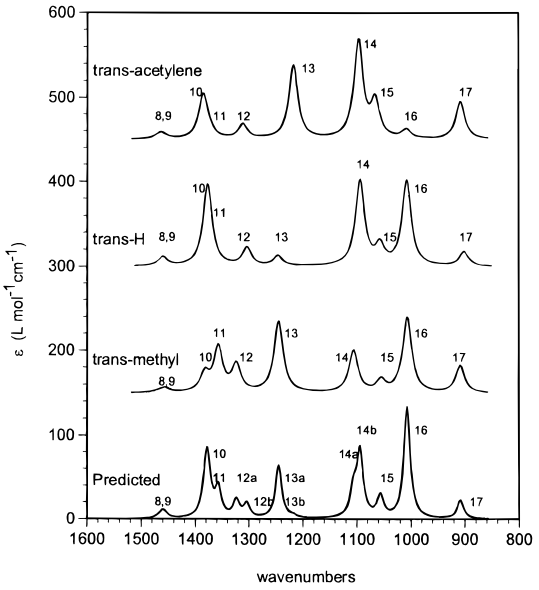

Figure 2. Ab initio vibrational absorption spectra for three conformers of (*S*)-3-butyn-2-ol obtained with B3LYP/6-31G* basis set. The spectra were simulated with Lorentzian band shapes and 10 cm^{-1} half-widths and frequencies were multiplied with 0.96. The labels on the traces are the conformation labels (Figure 1). The predicted spectrum (bottom trace) is obtained by adding the population-weighted absorption spectra of all conformers. The numbers for the peaks in top three spectra correspond to the band numbers listed in Table 4; the numbers in the bottom spectrum correspond to the numbers in Table 5.

The experimental absorption spectrum (see Figure 4 and Table 5) at lower concentration contains 12 bands at ∼1450, 1445, 1377, 1358, 1329, a shoulder at 1316, 1256, 1187, 1111, 1078, 1026, and 922 cm^{-1} in the 1500−900 cm^{-1} region. The weak absorption band at 1078 cm^{-1} appears also to contain a shoulder on the lower frequency side. As the concentration is increased,

TABLE 4: Ab Initio Unscaled Frequencies (cm^{-1}), Absorption and VCD Intensities, and Potential Energy Distribution (PED) for (*S*)-3-Butyn-2-ol

	trans-acetylene				*trans*-H				*trans*-methyl			
no.	freq[a]	A^a	R^a	PED[b]	freq[a]	A^a	R^a	PED[b]	freq[a]	A^a	R^a	PED[b]
1	3736	9.64	−1.72	5	3730	13.83	3.00	5	3743	15.79	−1.69	5
2	3496	48.67	0.16	7	3494	50.4	0.14	7	3494	50.22	−0.52	7
3	3148	19.06	−2.97	9, 10, 8	3142	22.10	1.15	8, 10, 9	3151	19.63	−3.91	9, 10, 8
4	3121	27.91	2.33	10, 8, 9	3127	29.75	0.33	9, 10, 8	3147	19.78	3.61	8, 10, 9
5	3051	23.10	3.37	8, 10, 9	3067	15.53	−1.30	3, 10, 8	3069	13.83	0.84	8, 10, 9
6	2978	48.85	0.78	3	3055	12.93	−0.59	9, 10, 8	2980	49.83	3.39	3
7	2248	2.25	0.07	6, 2	2232	1.13	−0.09	6, 2, 7	2232	1.08	−0.13	6, 2
8	1527	3.15	−3.46	19, 20, 16	1521	0.29	0.92	19, 16, 18	1526	1.42	3.04	19, 20
9	1519	3.25	1.34	20, 19	1519	7.26	−0.10	20, 19	1514	3.41	−2.09	20, 17
10	1442	36.86	−21.24	15, 21, 12	1433	64.63	−31.54	12, 21, 15	1438	15.16	15.38	20, 17, 18
11	1431	5.17	−2.35	18, 17, 20	1429	6.16	0.63	20, 18, 16	1412	37.47	61.80	21, 15, 16
12	1364	12.16	−19.04	12, 15	1356	15.43	13.97	15, 12, 16	1377	22.63	4.48	12, 15
13	1267	63.62	34.45	15, 21, 12	1296	8.42	11.64	21, 15, 12	1295	60.49	−56.78	21, 17, 12
14	1141	83.31	−4.24	18, 1, 17	1138	72.58	−38.70	16, 18, 1	1150	35.47	−9.71	18, 1, 16
15	1108	30.75	18.66	17, 16, 4	1099	16.11	−17.07	4, 17, 1	1097	9.59	31.40	17, 15, 16
16	1048	7.23	−0.48	4, 1, 16	1048	72.25	−4.40	17, 1, 16	1047	64.04	−12.91	4, 1, 21
17	943	32.36	5.67	18, 2, 1	937	12.12	8.13	18, 1, 2	945	22.95	3.80	1, 18, 2
18	813	2.05	−9.40	2, 4, 17	806	8.28	21.60	2, 4, 17	819	5.57	4.29	2, 17, 4
19	656	37.78	−2.53	23, 27	647	41.48	0.27	27, 23	646	39.97	−3.41	27, 23, 26
20	612	52.02	−10.33	27, 23	610	57.71	−1.66	23, 27	613	52.15	−6.85	23, 27
21	577	2.69	−6.80	13, 26, 22	572	6.44	1.43	13, 22	579	2.90	−14.03	13, 26, 12
22	543	4.31	10.27	14, 22, 13	544	11.20	9.02	14, 13, 26	537	9.29	−8.16	14, 22, 13
23	396	4.87	6.95	11, 18, 14	396	16.01	8.08	11, 14, 18	393	10.13	22.08	11, 14, 18
24	292	20.22	65.62	25, 26, 24	309	102.05	−20.31	24, 22, 11	314	125.72	−15.63	24
25	261	96.86	−80.65	24, 25	270	7.87	44.01	25, 22, 24	267	4.61	−5.47	25, 26, 13
26	229	13.29	2.44	26, 15, 25	211	7.14	−3.25	22, 14, 15	220	1.78	4.88	26, 25, 14
27	189	2.85	4.17	22, 14, 13	182	1.13	−1.94	26, 14, 13	175	1.08	−0.41	22, 14, 13

[a] Frequencies in cm^{-1}, absorption intensities (*A*) in km/mol, and rotational strengths (*R*) in 10^{-44} esu^2 cm^2 obtained with the B3LYP/6-31G* basis set. [b] Internal coordinates with largest contributions to PED; for internal coordinate definition see Table 3.

TABLE 5: Comparison of Predicted and Observed Frequencies for 3-butyn-2-ol

band no.[a]	expt (cm^{-1})[b]	pred (cm^{-1})[c,d]	calc[c,e] (cm^{-1})	assignment
8	1450	1465	1526	HCH bend
9	1445	1458	1519	HCH bend
10	1377	1377	1433	$O_2C_1H_7$ bend, $C_1O_2H_3$ bend
11	1358	1360	1412	$C_1O_2H_3$ bend
12a	1329	1322	1377	$O_2C_1H_7$ bend
12b	1316	1305	1356	$H_7C_1C_4$ bend
13a	1256	1246	1296	$C_1O_2H_3$ bend
13b	1187	1218	1267	$H_7C_1C_4$ bend
14a	1111	1105	1150	C_1C_8H bend
14b		1095	1138	C_1C_8H bend
15	1078	1057	1097	C_1C_8H bend, C_1C_8 stretch
16	1026	1007	1048	C_1C_8H bend, C_1C_8 stretch
17	922	908	945	CO stretch

[a] These numbers derived from those in Table 4. [b] Experimental frequencies obtained from the absorption spectrum at concentration of 0.103 M. [c] Band positions from the simulated spectra with populations given in Table 1. [d] Ab initio frequencies scaled with 0.96. [e] Unscaled ab initio frequencies.

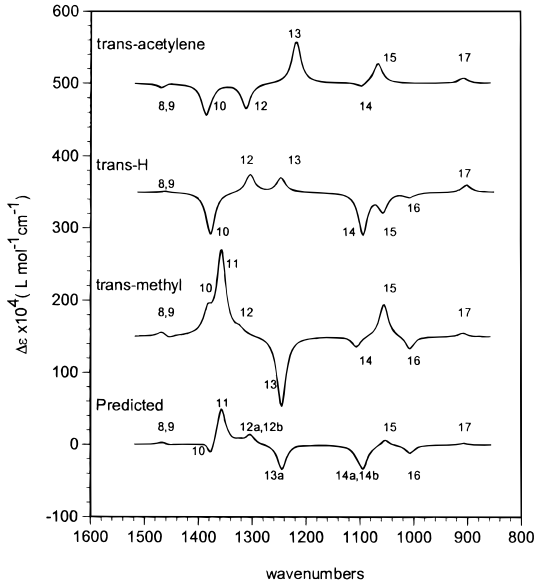

Figure 3. Ab initio VCD spectra for three conformers of (*S*)-3-butyn-2-ol obtained with the B3LYP/6-31G* basis set. The spectra were simulated with Lorentzian band shapes and 10 cm^{-1} half-widths and frequencies were multiplied by 0.96. The labels on the traces are the conformation labels (Figure 1). The predicted spectrum (bottom trace) is obtained by adding the population-weighted VCD spectra of all conformers. The numbers for the peaks in the top three spectra correspond to the band numbers listed in Table 4; the numbers in the bottom spectrum correspond to the numbers in Table 5.

new bands at 1280 and 1410 cm^{-1} appear, and the band at 1026 cm^{-1} shifts to higher frequency (1036 cm^{-1}) and it is broadened, and the band at 1358 cm^{-1} decreases in intensity. On the basis of vibrational analysis, the experimental absorption bands at 1377, 1358, and 1256 cm^{-1} have major contribution from H−O−C bending internal coordinate. Thus, the intensity changes, and new bands, seen in this region at higher concentrations are consistent with the assumption that intermolecular hydrogen bonding dominates at higher concentrations. It is possible that the new bands at 1280 and 1410 cm^{-1} seen at higher concentration may correspond to the bands at 1256 and 1377 cm^{-1} seen at lower concentration because this is consistent

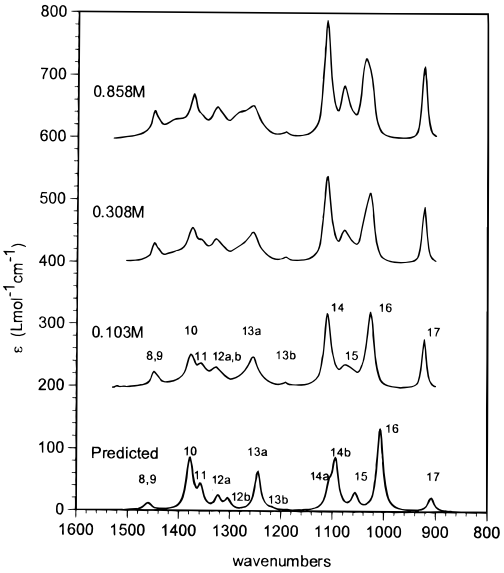

Figure 4. Comparison of the experimental absorption spectra of (−)-3-butyn-2-ol at different concentrations (top three traces) with the predicted (population weighted) absorption (bottom trace) obtained with B3LYP/6-31G* basis set. The spectra were simulated with Lorentzian band shapes and 10 cm^{-1} half-widths and frequencies were multiplied by 0.96. The labels on the top three traces give the concentration employed for the experimental spectra. The numbers for the peaks correspond to the band numbers listed in Table 5.

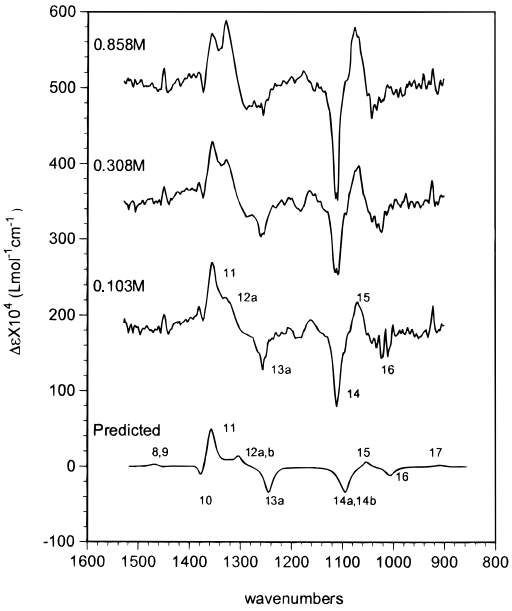

Figure 5. Comparison of the experimental VCD spectra of (−)-3-butyn-2-ol at different concentrations (top three traces) with the predicted (population weighted) VCD of (bottom trace) obtained with B3LYP/6-31G* basis set. The spectra were simulated with Lorentzian band shapes and 10 cm^{-1} half-widths and frequencies were multiplied by 0.96. The labels on the top three traces give concentration employed for the experimental spectra. The numbers for the peaks correspond to the band numbers listed in Table 5.

with the view that upon intermolecular hydrogen bonding the C−O−H bending vibrations shift to higher frequencies.[20] The changes observed for the experimental 1026 cm^{-1} absorption band can be rationalized by the hypothesis that at dilute concentrations nearly equal amounts of *trans*-H and *trans*-methyl conformations are present while at higher concentrations, where intermolecular hydrogen bonding becomes important, *trans*-methyl conformation dominates (vide infra). The *trans*-methyl

conformation is favorable for intermolecular hydrogen bonding because in this conformation the bulky CH_3 group does not hinder such bonding. The mode composition for the corresponding calculated band of *trans*-H conformation (band no. 16 in Table 4) does not have a predominant contribution from the H−O−C bending coordinate, but that for *trans*-methyl conformation has a predominant contribution from the H−O−C bending coordinate. So, as the concentration increases, and the population of *trans*-methyl conformation increases, the contribution from the H−O−C bending coordinate to the observed experimental band at 1026 cm^{-1} increases; then intermolecular hydrogen bonding causes this band to shift to higher frequency at 1036 cm^{-1}.

At lower concentrations, intermolecular hydrogen bonding is expected to be less significant, so the experimental spectra at lower concentrations are expected to be closer to those predicted for isolated molecules. This in fact is evident in Figure 4, where the population-weighted theoretical absorption spectrum compares favorably to the experimental absorption spectrum obtained at 0.103 M concentration, but not to that at 0.858 M.

The experimental VCD spectrum (see Figure 5) at concentration of 0.103 M clearly shows six bands at 1356 (+), 1329 (+), 1263 (−), 1111 (−), 1065 (+), and 1014 (−) cm^{-1}. The weak VCD signals seen in the 1200−1140 cm^{-1} region are not reliable. As the concentration is increased the relative intensity of the positive VCD band at 1329 cm^{-1} increases over that of the VCD band at 1356 cm^{-1}, and the negative VCD band at 1263 cm^{-1} is decreased and broadened. The population-weighted theoretical VCD spectrum matches better with the experimental VCD spectrum obtained at the 0.103 M concentration. At higher concentrations, the relative intensities of the two positive bands at 1356 and 1329 cm^{-1} change and the experimental VCD spectrum at 0.858 M concentration (Figure 5) compares more favorably to that predicted for the *trans*-methyl conformation shown in Figure 3 (with some intermolecular hydrogen bonding effects that are not present in the predicted spectrum).

Thus, based on the absorption and VCD spectra obtained at different concentrations, and the corresponding theoretical spectra, it appears that the relative populations predicted for isolated 3-butyn-2-ol are applicable to the solution phase sample at lower concentrations. At higher concentrations, 3-butyn-2-ol appears to adopt *trans*-methyl conformation, which is in contrast to the nearly equal populations of *trans*-H and *trans*-methyl conformations at lower concentrations. These observations are in agreement with the optical rotation calculations,[14] where the negative optical rotation for (*S*)-3-butyn-2-ol liquid was predicted to originate from the *trans*-methyl conformation.

Summary

The comparison of experimental and ab initio predicted absorption and VCD spectra indicate that (a) at low concentrations in CCl_4 solutions, 3-butyn-2-ol is present in nearly equal amounts of *trans*-H and *trans*-methyl conformations where intramolecular hydrogen bonding between O−H and π-electrons is present; (b) at higher concentrations, 3-butyn-2-ol appears to be present predominantly in the *trans*-methyl conformation, which is favorable for intermolecular hydrogen bonding.

Acknowledgment. Grants from NSF (CHE9707773) and Vanderbilt University are gratefully acknowledged.

References and Notes

(1) Stinson, S. C. *Chem. Eng. News* **1993**, *71*(39), 38.
(2) Nakanishi, K.; Berova, N.; Woody, R. W. *Circular dichroism: Principles and Applications*; VCH Publishers: New York, 1994.
(3) Polavarapu, P. L.; Zhao, C. *Chem. Phys. Lett*. **1998**, *296*, 105.
(4) (a). Holzwarth, G.; Hsu, E. C.; Mosher, H. S.; Faulkner, T. R.; Moscowitz, A. *J. Am. Chem. Soc.* **1974**, *96*, 251. (b). Nafie, L. A.; Keiderling, T. A.; Stephens, P. J. *J. Am. Chem. Soc*. **1976**, *98*, 2715.
(5) Barron, L. D. *Molecular Light Scattering and Optical Activity*; Cambridge University Press: Cambridge, UK, 1982.
(6) Polavarapu, P. L.; Zhao, C.; Ramig, K. *Tetrahedron: Asymmetry* **1999**, *10*, 1099.
(7) Polavarapu, P. L.; Cholli, A.; Vernice, G. *J. Am. Chem. Soc*. **1992**, *114*, 4, 10953.
(8) (a) Polavarapu, P. L.; Cholli, A. L.; Vernice, G. *J. Pharm. Sci*. **1993**, *82*, 791. (b) Polavarapu, P. L.; Cholli, A. L.; Vernice, G. *J. Pharm. Sci*. **1997**, *86*, 267. (c) Polavarapu, P. L.; Zhao, C.; Cholli, A. L.; Vernice, G. *J. Phys. Chem. B* **1999**, *103*, 6127; Zhao, C.; Polavarapu, P. L.; Grosenick, H.; Schurig, V. *J. Mol. Struct*., in press.
(9) Costante, J.; Hecht, L.; Polavarapu, P. L.; Collet, A.; Barron, L. D. *Angew. Chem., Int. Ed*. **1997**, *36*, 885.
(10) Ashvar, C. S.; Stephens, P. J.; Eggiman, T.; Wieser, H. *Tetrahedron: Asymmetry* **1998**, *9*, 1107.
(11) Toda, F. Jpn. Kokai Tokkyo Koho A2 **1987**, 27 (patent JP6224653); *Chem. Abstr.* **1987**, *108*, 204218.
(12) Landor, S. R.; Miller, B. J.; Tatchell, A. R. *J. Chem. Soc. (C)* **1971**, 2339.
(13) Marstokk, K.-M.; Mollendal, H. *Acta Chem. Scandinavica A* **1985**, *39*, 639.
(14) Polavarapu, P. L.; Chakrabory, D. *Chem. Phys*. **1999**, *240*, 1.
(15) Becke, A. D. *J. Chem. Phys*. **1993**, *98*, 1372, 5648.
(16) Cheeseman, J. R.; Frisch, M. J.; Devlin, F. J.; Stephens, P. J. *Chem. Phys. Lett.* **1996**, *252*, 211.
(17) *Gaussian 98*, Revision A.3; Frisch, M. J.; Trucks, G. W.; Schlegel, H. B.; Scuseria, G. E.; Robb, M. A.; Cheeseman, J. R.; Zakrzewski, V. G.; Montgomery, Jr., J. A.; Stratmann, R. E.; Burant, J. C.; Dapprich, S.; Millam, J. M.; Daniels, A. D.; Kudin, K. N.; Strain, M. C.; Farkas, O.; Tomasi, J.; Barone, V.; Cossi, M.; Cammi, R.; Mennucci, B.; Pomelli, C.; Adamo, C.; Clifford, S.; Ochterski, J.; Petersson, G. A.; Ayala, P. Y.; Cui, Q.; Morokuma, K.; Malick, D. K.; Rabuck, A. D.; Raghavachari, K.; Foresman, J. B.; Cioslowski, J.; Ortiz, J. V.; Stefanov, B. B.; Liu, G.; Liashenko, A.; Piskorz, P.; Komaromi, I.; Gomperts, R.; Martin, R. L.; Fox, D. J.; Keith, T.; Al-Laham, M. A.; Peng, C. Y.; Nanayakkara, A.; Gonzalez, C.; Challacombe, M.; Gill, P. M. W.; Johnson, B.; Chen, W.; Wong, M. W.; Andres, J. L.; Gonzalez, C.; Head-Gordon, M.; Replogle, E. S.; Pople, J. A. Gaussian, Inc.: Pittsburgh, PA, 1998.
(18) Hehre, W. J.; Radom, L.; Schleyer, P. V. R.; Pople, J. A. *Ab initio Molecular Orbital Theory*; John Wiley & Sons: New York, 1986.
(19) Schachtschneider, J. H. "Vibrational analysis of polyatomic molecules"; Reports 231/64 and 57/65, Shell Development Co., Houston, TX 1962.
(20) Sun, Z.; Wang, F.; Tang, Z.; Yan, G. *Chin. J. At. Mol. Phys.* **1995**, *12*, 375. Lozynski, M.; Roszak, D. R.; Mack, H.-G. *J. Phys. Chem. A* **1998**, *102*, 2899.